

# Upregulation of the PI3K/Akt Pathway in the Tumorigenesis of Canine Thyroid Carcinoma

M. Campos, M.M.J. Kool, S. Daminet, R. Ducatelle, G. Rutteman, H.S. Kooistra, S. Galac, and J.A. Mol

**Background:** Information on the genetic events leading to thyroid cancer in dogs is lacking.

**Hypothesis/Objectives:** Upregulation of the PI3K/Akt pathway has an important role in the tumorigenesis of thyroid carcinoma in dogs.

**Animals:** Fifty-nine dogs with thyroid carcinoma and 10 healthy controls.

**Methods:** Quantitative RT-PCR was performed for *VEGFR-1*, *VEGFR-2*, *EGFR*, *PIK3CA*, *PIK3CB*, *PDPK1*, *PTEN*, *AKT1*, *AKT2*, *COX-2*, and *CALCA*. Mutation analysis was performed for known hotspots of *RAS* (*N*, *K*, *H*), *PIK3CA*, *BRAF*, *RET*, and for the entire coding region of *PTEN*.

**Results:** Forty-three dogs (73%) had follicular cell thyroid carcinoma (FTC) and 16 dogs (27%) had medullary thyroid carcinoma (MTC). The relative mRNA expressions of *VEGFR-1* ( $P < .001$ ), *VEGFR-2* ( $P = .002$ ), *PDPK1* ( $P < .001$ ), *AKT1* ( $P = .009$ ), and *AKT2* ( $P < .001$ ) were increased in FTC, and those of *EGFR* ( $P < .001$ ), *VEGFR-1* ( $P = .036$ ), and *PIK3CA* ( $P = .019$ ) were increased in MTC when compared to normal thyroid glands. Mutation analysis of *K-RAS* identified 2 activating missense mutations, which also have been described in thyroid cancer of humans. A G12R substitution was present in 1 FTC and an E63K substitution was present in 1 MTC. No functional mutations were found in the sequenced regions of *H-RAS*, *N-RAS*, *PIK3CA*, *BRAF*, *RET*, and *PTEN*.

**Conclusions and Clinical Importance:** The increased expression of several genes associated with PI3K/Akt signaling suggests the involvement of this pathway in the pathogenesis of thyroid carcinoma in dogs, warranting further research on pathway activation and gene amplification. The mutations most frequently associated with thyroid cancer in humans are rare in dogs.

**Key words:** C-cell; Dog; Follicular; Medullary; RAS.

Thyroid cancer represents 10–15% of all head and neck neoplasms in the dog.<sup>1</sup> Ninety percent of thyroid tumors in dogs detected clinically are malignant and can be classified as either follicular cell thyroid carcinoma (FTC), which arises from thyroid follicular cells, or medullary thyroid carcinoma (MTC), which arises from the parafollicular cells (C-cells).<sup>2</sup> Differentiated FTC (follicular, compact, follicular-compact, papillary) in dogs is remarkably similar in histology and biologic behavior to follicular thyroid carcinoma in humans.<sup>3</sup> Likewise, the morphologic, cytochemical, and immunohistochemical features of canine MTC also resemble human MTC.<sup>4</sup>

Information on the genetic pathogenesis of thyroid cancer in dogs is scarce. Oncogenic gene amplification or copy number gain are prominent genetic mechanisms causing thyroid gland tumorigenesis in humans.<sup>5</sup>

From the Department of Medicine and Clinical Biology of Small Animals, (Campos, Daminet); the Department of Pathology, Bacteriology and Poultry Diseases, (Ducatelle), Faculty of Veterinary Medicine, Ghent University, Merelbeke, Belgium; and Department of Clinical Sciences of Companion Animals, Faculty of Veterinary Medicine, Utrecht University, Utrecht, The Netherlands (Kool, Rutteman, Kooistra, Galac, Mol).

This work was performed at Utrecht University, The Netherlands.

Corresponding author: M. Campos, Alfort National Veterinary School, Paris-Est University, 7 avenue du Général de Gaulle, 94704 Maisons-Alfort, France; e-mail: miguel.campos@vet-alfort.fr.

Submitted February 27, 2014; Revised July 14, 2014; Accepted July 22, 2014.

Copyright © 2014 by the American College of Veterinary Internal Medicine

DOI: 10.1111/jvim.12435

## Abbreviations:

AKT1	v-akt murine thymoma viral oncogene homolog 1
AKT2	v-akt murine thymoma viral oncogene homolog 2
APES	3-aminopropyltriethoxysilane
bp	base pairs
BRAF	v-raf murine sarcoma viral oncogene homolog B
CALCA	calcitonin-related polypeptide alpha
COX-2	cyclooxygenase-2
CT	cycle threshold
EGFR	epidermal growth factor receptor
FF-PE	formalin-fixed paraffin-embedded
FTC	follicular cell thyroid carcinoma
Fw	forward
GDP	guanosine diphosphate
GTPase	guanosine triphosphatase
GTP	guanosine triphosphate
HE	hematoxylin and eosin
HPRT	hypoxanthine phosphoribosyltransferase 1
H-RAS	Harvey rat sarcoma viral oncogene homolog
IHC	immunohistochemistry
K-RAS	Kirsten rat sarcoma viral oncogene homolog
MAPK	mitogen-activated protein kinase
MTC	medullary thyroid carcinoma
N-RAS	neuroblastoma RAS viral (v-ras) oncogene homolog
PDPK1	3-phosphoinositide-dependent protein kinase-1
PI3K	phosphatidylinositol-3-kinase
PIK3CA	phosphatidylinositol-4,5-bisphosphate 3-kinase catalytic subunit alpha
PIK3CB	phosphatidylinositol-4,5-bisphosphate 3-kinase catalytic subunit beta
PTEN	phosphatase and tensin homolog
qPCR	quantitative RT-PCR
RET	rearranged during transfection
RPS5	ribosomal protein S5
RTK	receptor tyrosine kinase
Rv	reverse

This is especially true for genes involved in the phosphatidylinositol-3-kinase (PI3K)/Akt pathway (Fig 1). Prominent examples of such genes include *EGFR*, *VEGFR-1*, *VEGFR-2*, *PIK3CA*, *PIK3CB*, *AKT1*, *AKT2*, and *PDPK1*.<sup>6</sup> Epidermal growth factor receptor, *VEGFR-1* and *VEGFR-2* are important regulators of both mitogen-activated protein kinase (MAPK) and PI3K/Akt signaling pathways. However, copy number gains in these receptor tyrosine kinase (RTK) genes in human thyroid cancer are particularly associated with PI3K/Akt pathway activation, which is the major pathway involved in the pathogenesis of follicular thyroid carcinoma in humans.<sup>6-8</sup> An important and expected consequence of gene amplification or pathway activation is increased mRNA and protein expression and consequent aberrant activation of downstream signaling.<sup>6</sup> The mRNA expression of the RTKs and downstream effectors involved in PI3K/Akt signaling may provide valuable information regarding gene amplification and pathway activation, and has not yet been investigated in thyroid tumors in dogs.

Several reports have suggested that the PI3K/Akt signaling pathway regulates the expression of cyclooxygenase-2 (Cox-2).<sup>9,10</sup> Cox-2 functions downstream of Akt, and increased Akt activity is crucial for *COX-2* overexpression in apoptotic-resistant cells.<sup>9</sup> Cox-2 mRNA expression could therefore also be used to infer the activity of the PI3K/Akt pathway.

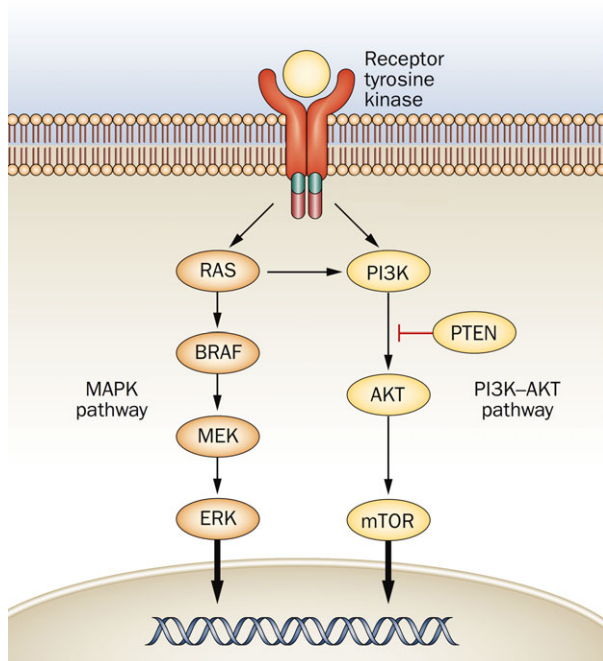


**Fig 1.** Simplified schematic illustration of PI3K/Akt and mitogen-activated protein kinase (MAPK) signaling pathways in thyroid cancer. These pathways are involved in propagation of signals from various receptor tyrosine kinases into the nucleus, and they regulate multiple cell processes including proliferation, differentiation, and survival. Adapted by permission from Macmillan Publishers Ltd: [Nature Reviews Endocrinology], copyright (2011).<sup>40</sup>

One of the most important genetic events described in human follicular thyroid carcinoma is point mutations in 1 of the 3 *RAS* genes.<sup>6</sup> The *RAS* genes (*N*, *K*, and *H-RAS*) encode membrane-bound intracellular proteins involved in cellular signal transduction. These proteins act as on/off switches, relaying extracellular signals to the cytoplasmic signaling cascades of the MAPK and PI3K/Akt pathways, which control cellular proliferation, differentiation, and survival (Fig 1).<sup>11</sup> In many cancers in humans, point mutations in exon 1 (codons 12 and 13) or exon 2 (codons 59 and 61) fix *RAS* proteins in a permanently activated state, promoting uncontrolled cellular division and malignant transformation.<sup>12</sup> Although *RAS* is a classical dual activator of both PI3K/Akt and MAPK signaling, *RAS* mutations seem to preferentially activate the PI3K/Akt pathway in thyroid gland tumorigenesis.<sup>6</sup> Mutations in *RAS* genes have not yet been investigated in thyroid tumors in dogs.

Point mutations in the tumor suppressor gene phosphatase and tensin homolog (*PTEN*) and in the phosphatidylinositol-4,5-bisphosphate 3-kinase catalytic subunit alpha (*PIK3CA*) gene also are reported in human follicular thyroid carcinoma.<sup>5</sup> Because *PTEN* has an inhibitory effect on the PI3K/Akt pathway, inactivating mutations or deletions in *PTEN* lead to PI3K/Akt pathway activation and promote tumorigenesis.<sup>13</sup> Activating point mutations in the *PIK3CA* gene lead to a constitutively activated protein that also activates PI3K/Akt pathway. Mutations in *PTEN* or *PIK3CA* have not been evaluated in thyroid cancer in dogs.

The most important genetic alterations in papillary thyroid carcinoma in humans are activating point mutations of v-raf murine sarcoma viral oncogene homolog B (*BRAF*) which lead to activation of MAPK signaling pathway.<sup>14</sup> Mutations in *BRAF* have not been investigated in thyroid tumors of dogs.

The principal molecular mechanism underlying human MTC is aberrant activation of *RET* (rearranged during transfection), a RTK which signals through the PI3K/Akt and MAPK pathways.<sup>15,16</sup> Germ line *RET* mutations are responsible for the hereditary forms of human MTC, whereas somatic *RET* mutations are present in approximately 50% of patients with sporadic MTC.<sup>17</sup> In addition, *RAS* mutations have been reported in up to 68% of human MTCs without *RET* mutations.<sup>18</sup> In the only case report of canine familial MTC, no mutation was found after complete sequencing of *RET*.<sup>19</sup> The genetic events underlying sporadic canine MTC have not yet been investigated.

Immunohistochemistry (IHC) for thyroglobulin, calcitonin, or markers of neuroendocrine tissue aids differentiation of canine FTC and MTC.<sup>4</sup> mRNA expression of the gene encoding calcitonin (calcitonin-related polypeptide alpha—*CALCA*) has not yet been evaluated in dogs with thyroid tumors and also may help differentiate FTC from MTC.

We hypothesized that upregulation of the PI3K/Akt pathway has an important role in the tumorigenesis of thyroid carcinoma in dogs. The first aim of our study

was to determine if there is increased mRNA expression of selected genes involved in the PI3K/Akt signaling pathway by performing quantitative analysis of mRNA expression of those genes. The second aim of our study was to investigate hotspot mutations in selected genes involved in the PI3K/Akt and MAPK signaling pathways by sequencing selected regions of those genes that correspond to the human hotspots. The third aim of our study was to determine if mRNA expression of *CALCA* differs among FTC, MTC, and normal thyroid gland in dogs by performing quantitative analysis of *CALCA* gene expression and comparing it among the 3 groups.

## Materials and Methods

### Case Selection

The medical record databases of the Companion Animal Clinics of Ghent and Utrecht Universities were searched for dogs diagnosed with thyroid carcinoma from 1986 to 2013. Patients from which frozen ( $-80^{\circ}\text{C}$ ) tumor samples were not available were excluded.

### Thyroid Specimens

In total, 59 thyroid tumors (43 FTCs, 16 MTCs) and 10 normal thyroid glands (whole tissue explants) were analyzed. Tumor samples were collected from the Departments of Pathology of Ghent and Utrecht Universities. Samples were collected immediately after surgical or necropsy removal, part formalin-fixed paraffin-embedded (FF-PE), and part snap-frozen in liquid nitrogen and conserved at  $-80^{\circ}\text{C}$  until total RNA extraction.

### Histopathology

All HE-stained slides were reviewed by a board-certified pathologist (RD). All tumors were classified according to World Health Organization classification of canine thyroid tumors.<sup>20</sup> The distinction between adenoma and carcinoma was based on histologic evidence of capsular invasion, vascular invasion, or metastases.

### Immunohistochemistry

Five- $\mu\text{m}$  sections from each FF-PE block were prepared on 3-aminopropyltriethoxysilane-coated slides. IHC was performed as previously described.<sup>21</sup> For calcitonin IHC, sections were incubated overnight with the primary antibody (rabbit polyclonal antibody A0576<sup>a</sup> diluted 1 : 400) in a humidity chamber at  $4^{\circ}\text{C}$ . IHC was performed in 2 batches.

All sections were examined by the same investigator (MC). Thyroid tumors positive for calcitonin were classified as MTC and thyroid tumors negative for calcitonin were classified as FTC.<sup>4</sup> To verify the accuracy of our classification, the subset of tumors positive for calcitonin also was stained for thyroglobulin (rabbit polyclonal antibody A0251<sup>a</sup> diluted 1 : 800) in an automated immunostainer<sup>a</sup> (S/N S38-7410-01). Calcitonin and thyroglobulin immunolabeling were not quantified. For both stains, the tumors were considered positive when the cytoplasm of neoplastic cells exhibited a fine granular staining pattern with cell-to-cell variation. Normal thyroid gland was used as control in each batch. Tumors with neoplastic cells immunopositive for both thyroglobulin and calcitonin were classified as rare variants

of MTC with expression of thyroglobulin. However, in no tumor section were neoplastic cells observed to be immunopositive for both antibodies.

### RNA Isolation and Reverse Transcription

Frozen tissue samples were disrupted and homogenized with a rotor-stator homogenizer and total RNA was isolated by using an RNeasy mini kit<sup>b</sup> according to the manufacturer's instructions. A DNase step was performed to avoid genomic DNA contamination. Purified RNA was quantified on a NanoDrop ND-1000 Spectrophotometer<sup>c</sup> and, in 12 samples (first 10 patients of inclusion period and 2 normal thyroid glands), its integrity was assessed on a Bioanalyzer Micro RNA Chip.<sup>d</sup> Exactly, 1,000 ng of total RNA of each sample were reverse transcribed into cDNA by using the iScript cDNA synthesis kit<sup>e</sup> according to the manufacturer's instructions.

### Primer Design

All PCR amplification primers (Table 1) were designed with Perl-primer v1.1.21 according to the parameters of the Bio-Rad iCycler manual and were ordered from Eurogentec.<sup>f</sup> All PCR primers also were used as sequence primers. When the region of interest could not be amplified in 1 stretch, overlapping primer pairs were used (Table 2). For quantitative RT-PCR (qPCR), temperature gradients were performed to determine the optimal annealing temperature of each primer pair and primer specificity was confirmed by melting curve analysis and sequence analysis of the PCR products (Table 3).

### PCR Amplification

PCR amplification was performed by using the Phusion Hot Start Flex DNA Polymerase<sup>g</sup> on a C-1000 Touch thermal cycler.<sup>c</sup> PCR products were evaluated by agarose gel electrophoresis to confirm expected product length.

PCR products were amplified for sequencing by using the Big-Dye Terminator version 3.1 Cycle Sequencing Kit<sup>h</sup> and filtrated using Sephadex G-50 Superfine.<sup>i</sup> Sequencing was performed with the ABI3130XL Genetic Analyzer<sup>h</sup> according to the manufacturer's instructions. The obtained sequences were compared to the consensus mRNA sequence using DNASTar Lasergene core suite SeqMan Pro.<sup>j,k</sup> All mutations affecting the amino acid sequence were confirmed by repeating RNA extraction, reverse transcription, and sequencing.

### Quantitative RT-PCR

After reverse transcription, qPCR analyses were performed on cDNA to determine and compare the levels of expression of *VEGFR-1*, *VEGFR-2*, *EGFR*, *PIK3CA*, *PIK3CB*, *PDPK1*, *PTEN*, *AKT1*, *AKT2*, *COX-2*, and *CALCA* in thyroid tumors and normal thyroid glands. To correct for differences in sample input, the expression levels were normalized to the expression of the reference genes ribosomal protein S5 (*RPS5*) and hypoxanthine phosphoribosyltransferase (*HPRT*), already proven to be stable in other canine tissues.<sup>22</sup> Furthermore, the stability (M-value) of the reference genes was verified.

Quantitative RT-PCR was performed on a CFX384 real-time PCR detection system.<sup>e</sup> Each qPCR reaction mixture consisted of 4- $\mu\text{L}$  cDNA (diluted 50 $\times$ ), 0.4  $\mu\text{L}$  of both the forward and the reverse primers, 5- $\mu\text{L}$  iQ SYBR Green Supermix<sup>e</sup> and 0.2- $\mu\text{L}$  MilliQ, for a final reaction volume of 10  $\mu\text{L}$ . The thermal cycles were performed as previously described.<sup>23</sup> A 4-fold reference

**Table 1.** PCR primers for amplification of canine *RAS* (*K*, *N*, *H*), *BRAF*, *PIK3CA*, *RET*, and *PTEN*. All positions are based on the mRNA sequence published on NCBI.

PCR Primers	Sequence (5'–3')	Location	Exons	T <sub>a</sub> (°C)	Product Length (bp)
<i>K-RAS</i> Fw18	ATAAACTTGTGGTAGTTGGAGC	18/39	1–3	62	463
<i>K-RAS</i> Rv480	GTATAGAAGGCATCGTCAACAC	459/480			
<i>N-RAS</i> Fw12	GGTCTCCAACCTTTCTCC	12/29	1–5	55	660
<i>N-RAS</i> Rv672	AGTGTCTTGTACATCACCA	653/672			
<i>H-RAS</i> Fw54	CCATGACGGAGTATAAGCTG	54/73	1–2	55	253
<i>H-RAS</i> Rv306	ATGGCAAATACACAGAGAAAAG	286/306			
<i>BRAF</i> Fw1555	CGACAGACTGCACAGGGCATGG	1,555/1,573	13–16	55	372
<i>BRAF</i> Rv1926	CCGTACCTTACTGAGATCTGGAG	1,904/1,926			
<i>PIK3CA</i> Fw1504	TGCTGAACCCTATTGGTG	1,504/1,521	8–12	55	450
<i>PIK3CA</i> Rv1953	TACAGTCCAGAAGCTCCA	1,936/1,953			
<i>PIK3CA</i> Fw2872	TGGGAATTGGAGATCGTC	2,872/2,889	19–21	55	554
<i>PIK3CA</i> Rv3425	CAGTCTTTGCCTGTTGAC	3,408/3,425			
<i>RET</i> Fw1600	AAGTGCGAGTGGAGACAG	1,600/1,617	9–15	62	1,055
<i>RET</i> Rv2654	GAAATCTTCATCTTCCGCC	2,635/2,654			
<i>PTEN</i> Fw76	TCCTCCTTCCTCTCCAG	76/92	1–6	55	748
<i>PTEN</i> Rv823	TGAACTTGTCTTCCCGTC	806/823			
<i>PTEN</i> Fw719	CAATGTTCAAGTGGCGGA	719/735	6–8	55	742
<i>PTEN</i> Rv1460	CGAGATTGGTCAGGAAGAG	1,442/1,460			

*K-RAS*, Kirsten rat sarcoma viral oncogene homolog; *N-RAS*, neuroblastoma *RAS* viral (v-ras) oncogene homolog; *H-RAS*, Harvey rat sarcoma viral oncogene homolog; *BRAF*, v-raf murine sarcoma viral oncogene homolog B; *PIK3CA*, phosphatidylinositol-4,5-bisphosphate 3-kinase, catalytic subunit alpha; *RET*, ret proto-oncogene; *PTEN*, phosphatase and tensin homolog; Fw, forward; Rv, reverse; T<sub>a</sub>, optimal annealing temperature; bp: base pairs.

Accession numbers: *K-RAS*: XM\_003433561.2, *N-RAS*: NM\_001287065.1, *H-RAS*: NM\_001287069.1, *BRAF*: XM\_532749, *PIK3CA*: XM\_545208.4, *RET*: NM\_001197099.1, *PTEN*: NM\_001003192.1.

**Table 2.** Sequencing primers for canine *RAS* (*K*, *N*, *H*), *BRAF*, *PIK3CA*, *RET*, and *PTEN*. All positions are based on the mRNA sequence published on NCBI.

PCR Primers	Sequence (5'–3')	Location
<i>K-RAS</i> Rv355	ATTCCTACTAGGACCATAGGT	334/355
<i>N-RAS</i> Fw217	AAACAGGTGGTTATAGACGG	217/236
<i>N-RAS</i> Rv524	GTTTCAATGAATGGAATCCC	505/524
<i>H-RAS</i> Fw167	GACTCCTATCGGAAGCAAG	167/185
<i>H-RAS</i> Rv230	CTGTGTCCAGGATGTCCAG	212/230
<i>PIK3CA</i> Fw1549	CTCCATGCTTAGAGTTGGAG	1,549/1,568
<i>PIK3CA</i> Rv1815	CACAATAGTGTCTGTGGCTC	1,796/1,815
<i>PIK3CA</i> Fw3029	GATTAGTAAAGGAGCCCAGG	3,029/3,048
<i>PIK3CA</i> Rv3336	CATGCTGCTTAATGGTGTGG	3,317/3,336
<i>RET</i> Fw1906	GTGCTCTTCCTTCATCGT	1,906/1,925
<i>RET</i> Fw2221	AAAGGCAAAGCAGGATACAC	2,221/2,240
<i>RET</i> Rv1958	GTGGGCATTCTTGTTGATGC	1,977/1,958
<i>RET</i> Rv2278	GGGAAGCATTCTCTTCAGC	2,259/2,278
<i>PTEN</i> Fw475	CACTGTAAAGCTGGAAAGGG	475/494
<i>PTEN</i> Rv249	CCTGTATACGCCTCAAGTC	230/249
<i>PTEN</i> Rv595	TGTCTTGGTCTTACTTCC	576/595
<i>PTEN</i> Fw1158	TGTAGAGGAGCCATCAAACC	1,158/1,177
<i>PTEN</i> Rv1285	CAAAGGGTTCATTCTCTGGG	1,266/1,285

*K-RAS*, Kirsten rat sarcoma viral oncogene homolog; *N-RAS*, neuroblastoma *RAS* viral (v-ras) oncogene homolog; *H-RAS*, Harvey rat sarcoma viral oncogene homolog; *PIK3CA*, phosphatidylinositol-4,5-bisphosphate 3-kinase, catalytic subunit alpha; *RET*, ret proto-oncogene; *PTEN*, phosphatase and tensin homolog; Fw, forward; Rv, reverse.

Accession numbers: *K-RAS*: XM\_003433561.2, *N-RAS*: NM\_001287065.1, *H-RAS*: NM\_001287069.1, *PIK3CA*: XM\_545208.4, *RET*: NM\_001197099.1, *PTEN*: NM\_001003192.1.

standard dilution series using 10× diluted cDNA was included in every plate to assess reaction efficiency, and negative controls were used to assess the specificity of the reaction and check for contamination. Data were analyzed with CFX manager version

3.0.<sup>o</sup> Relative mRNA expression levels were calculated by relative quantitation and the fold-expression changes were determined by means of the 2<sup>-ΔΔCT</sup> method.<sup>24</sup> The maximum allowed cycle threshold (CT) value for calculations was 45.

**Table 3.** Quantitative RT-PCR primers for canine *VEGFR-1*, *VEGFR-2*, *EGFR*, *PIK3CA*, *PIK3CB*, *PDPK1*, *PTEN*, *AKT1*, *AKT2*, *COX-2*, *CALCA*, *RPS5*, and *HPRT*. All positions are based on the mRNA sequence published on NCBI.

qPCR Primers	Sequence (5'–3')	Location	$T_a$ (°C)	Product Length (bp)
<i>VEGFR-1</i> Fw189	GGCTCAGGCAAACCACAC	189/206	63	190
<i>VEGFR-1</i> Rv378	CCGGCAGGGGATGACGAT	361/378		
<i>VEGFR-2</i> Fw3606	GGAAGAGGAAGTGTGTGACCCC	3,606/3,627	64	181
<i>VEGFR-2</i> Rv3786	GACCATACCACTGTCCGTCTGG	3,765/3,786		
<i>EGFR</i> Fw2078	CTGGAGCATTCGGCA	2,078/2,092	53	108
<i>EGFR</i> Rv2185	TGGCTTTGGGAGACG	2,171/2,185		
<i>PIK3CA</i> Fw1269	CCTTGTTCTAATCCCAGGTG	1,269/1,288	58.5	134
<i>PIK3CA</i> Rv1402	GGACAGTGTTCCTTTAGC	1,383/1,402		
<i>PIK3CB</i> Fw2978	CCTTCAACAAAGATGCCC	2,978/2,995	62.5	142
<i>PIK3CB</i> Rv3119	CTATGTCTATCACC AATCCCA	3,099/3,119		
<i>PDPK1</i> Fw667	AGGTCTGAAC TTTACACGC	667/684	55.5	199
<i>PDPK1</i> Rv865	AGGGCATCATTCACAGG	846/865		
<i>PTEN</i> Fw1209	AGATGTTAGTGACAATGAACCT	1,209/1,230	62	102
<i>PTEN</i> Rv1310	GTGATTTGTGTGTGCTGATC	1,291/1,310		
<i>AKT1</i> Fw717	CACCGTGTGACCATGAATGAG	717/737	64	83
<i>AKT1</i> Rv799	TTCTCCTTGACCAGGATCACC	779/799		
<i>AKT2</i> Fw71	GGACCTTCCACGTAGACTC	71/89	60.5	195
<i>AKT2</i> Rv265	CATTCATGGTCACTTGGC	247/265		
<i>COX-2</i> Fw971	TTCCAGACGAGCAGGCTAAT	971/990	60	112
<i>COX-2</i> Rv1082	GCAGCTCTGGGTCAAACCTC	1,063/1,082		
<i>CALCA</i> Fw157	ATCATGGGCTTGTGGAAGTC	157/176	58.5	98
<i>CALCA</i> Rv254	AGAGCGGACCTGAATGGT	237/254		
<i>RPS5</i> Fw405	TCACTGGTGAGAACCCCTT	405/423	62.5	141
<i>RPS5</i> Rv545	CCTGATTCACACGGCGTAG	527/545		
<i>HPRT</i> Fw484	AGCTTGCTGGTGAAAAGGAC	484/503	58	104
<i>HPRT</i> Rv587	TTATAGTCAAGGGCATATCC	568/587		

*VEGFR-1*, vascular endothelial growth factor receptor-1; *VEGFR-2*, vascular endothelial growth factor receptor-2; *EGFR*, epidermal growth factor receptor; *PIK3CA*, phosphatidylinositol-4,5-bisphosphate 3-kinase, catalytic subunit alpha; *PIK3CB*, phosphatidylinositol-4,5-bisphosphate 3-kinase, catalytic subunit beta; *PDPK1*, 3-phosphoinositide dependent protein kinase-1; *PTEN*, phosphatase and tensin homolog; *AKT1*, v-akt murine thymoma viral oncogene homolog 1; *AKT2*, v-akt murine thymoma viral oncogene homolog 2; *COX-2*, cyclooxygenase-2; *CALCA*, calcitonin-related polypeptide alpha; *RPS5*, ribosomal protein S5; *HPRT*, hypoxanthine phosphoribosyltransferase; Fw, forward; Rv, reverse;  $T_a$ , optimal annealing temperature; bp: base pairs.

Accession numbers: *VEGFR-1*: AF262963.1, *VEGFR-2*: NM\_001048024.1, *EGFR*: XM\_533073.4, *PIK3CA*: XM\_545208.4, *PIK3CB*: XM\_534280.4, *PDPK1*: XM\_005621677.1, *PTEN*: NM\_001003192.1; *AKT1*: XM\_548000.4; *AKT2*: NM\_001012340.1, *COX-2*: NM\_001003354.1, *CALCA*: NM\_001003266.1, *RPS5*: XM\_533568.4, *HPRT*: AY\_283372.

### Sequencing

Sequencing was performed for human mutation hotspots of *K-*, *N-*, and *H-RAS* (exons 1 and 2),<sup>25</sup> *BRAF* (exon 15),<sup>26</sup> *PIK3CA* (exons 9 and 20),<sup>27</sup> *RET* (exons 8, 10, 11, 13–16),<sup>19</sup> and for the entire coding region of *PTEN* (hotspot exons 5–8)<sup>28</sup> on all 59 tumor samples and 2 normal thyroid glands.

### Statistical Analysis

Relative expression levels of *VEGFR-1*, *VEGFR-2*, *EGFR*, *PIK3CA*, *PIK3CB*, *PDPK1*, *PTEN*, *AKT1*, *AKT2*, *COX-2*, and *CALCA* were among thyroid tumors (FTC and MTC) and normal thyroid glands with the nonparametric independent-sample Kruskal-Wallis test because the data were not normally distributed.<sup>k</sup> The significance level was set at 5%. Dunn's test was used for multiple comparisons (adjusted *P* values are shown in the results section). The same procedure was used to compare the relative expression of reference genes between tumor samples and normal thyroid glands.

According to the mRNA expression of target genes, patients were grouped by means of unsupervised hierarchical clustering.<sup>1</sup> Unsupervised clustering was implemented by Pearson correlation for genes, and by Spearman correlation for samples.

### Results

Fifty-nine thyroid carcinomas were analyzed. Forty-three (73%) were FTC and 16 (27%) were MTC. Histologic subtypes of FTC included follicular (*n* = 8, 13%), follicular-compact (*n* = 11, 19%), compact (*n* = 18, 30%), papillary (*n* = 1, 2%), follicular-papillary (*n* = 1, 2%), and carcinosarcoma (*n* = 4, 7%).

#### mRNA Expression of PI3K/Akt Pathway-Related Genes

Relative mRNA expression was evaluated in 41 FTC, 15 MTC, and 10 normal thyroid glands (Fig 2). Relative expression levels of reference genes were not significantly different between thyroid tumors and normal thyroid glands.

The relative expression levels of *VEGFR-1* (*P* < .001), *VEGFR-2* (*P* = .002), *PDPK1* (*P* < .001), *AKT1* (*P* = .009), and *AKT2* (*P* < .001) were significantly higher in FTC than in normal thyroid glands. The relative expression levels of *EGFR* (*P* < .001), *VEGFR-1*

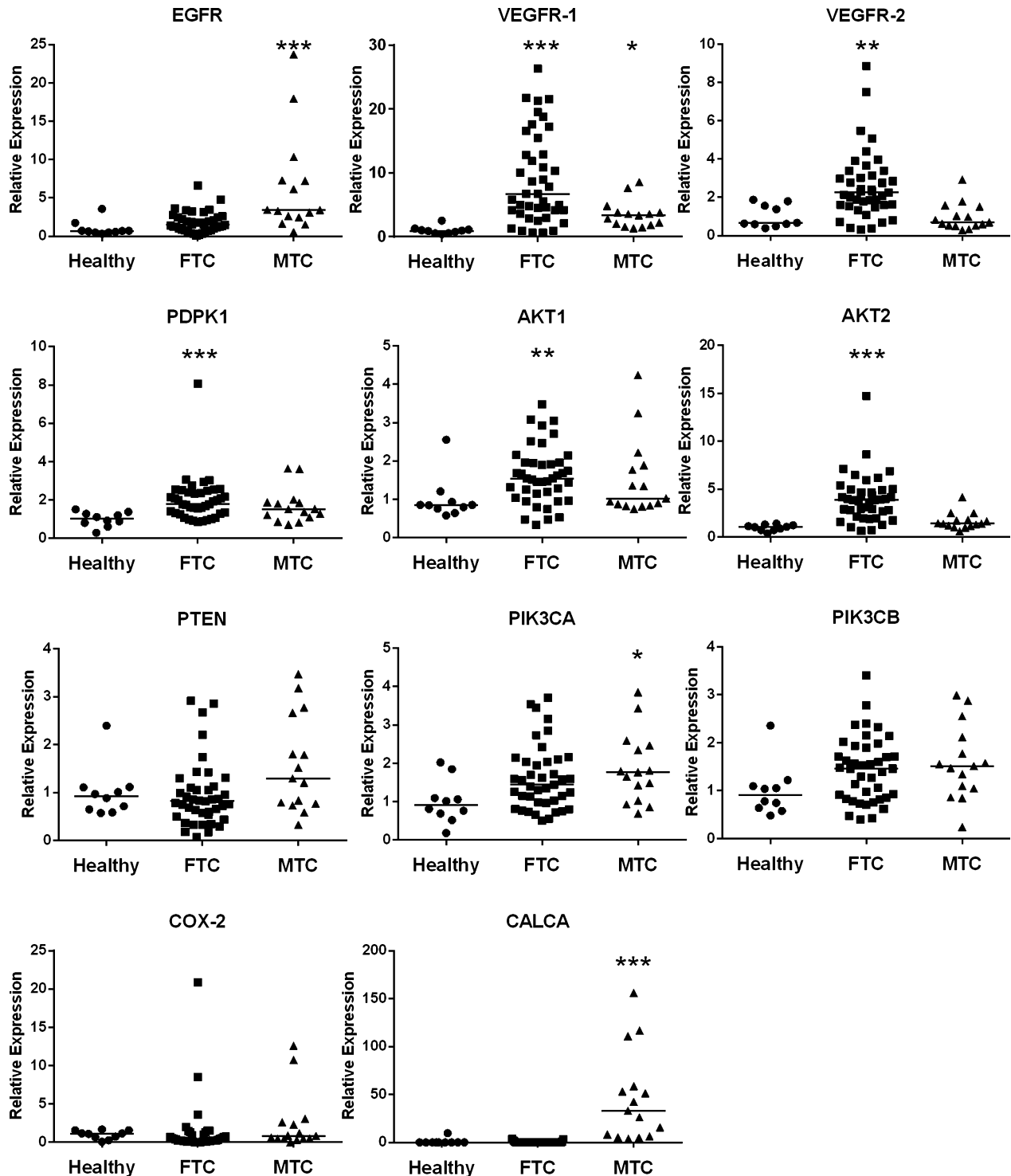


**Fig 2.** Dot plots representing the relative mRNA expression levels of *VEGFR-1*, *VEGFR-2*, *EGFR*, *PIK3CA*, *PIK3CB*, *PDK1*, *PTEN*, *AKT1*, *AKT2*, *COX-2*, and *CALCA* in canine normal thyroid gland (n = 10), FTC (n = 41) and MTC (n = 15). Significant differences between tumors and normal thyroid gland tissue are indicated with asterisks. FTC, follicular cell thyroid carcinoma; MTC, medullary thyroid carcinoma; *EGFR*, epidermal growth factor receptor; *VEGFR-1*, vascular endothelial growth factor receptor-1; *VEGFR-2*, vascular endothelial growth factor receptor-2; *PDK1*, 3-phosphoinositide dependent protein kinase-1; *AKT1*, v-akt murine thymoma viral oncogene homolog 1; *AKT2*, v-akt murine thymoma viral oncogene homolog 2; *PTEN*, phosphatase and tensin homolog; *PIK3CA*, phosphatidylinositol-4,5-bisphosphate 3-kinase, subunit alpha; *PIK3CB*, phosphatidylinositol-4,5-bisphosphate 3-kinase, catalytic subunit beta; *COX-2*, cyclooxygenase-2; *CALCA*: calcitonin-related polypeptide alpha; \* $P < .05$ ; \*\* $P < .01$ ; \*\*\* $P < .001$ .

( $P = .036$ ), *PIK3CA* ( $P = .019$ ), and *CALCA* ( $P < .001$ ) were significantly higher in MTC than in normal thyroid glands. Relative expression levels of *PTEN*, *PIK3CB*, and *COX-2* were not significantly different between thyroid tumors and normal thyroid glands. The relative expression levels of *CALCA* did not overlap between FTC (range, 0–3.6) and MTC (range, 3.9–156.1).

Unsupervised hierarchical clustering of the samples showed an almost perfect branching of normal thyroid glands, FTC, and MTC when all genes were included in the analysis (Fig 3). After omitting the relative expression of *CALCA*, clustering based on the remaining genes showed a more elaborate branching with normal thyroid gland enrichment in 1 branch, MTC enrichment in subsequent branching, and a final branch enriched in FTC.

Unsupervised hierarchical clustering of the genes showed separate branching for *CALCA*, *COX-2*, *EGFR*, and *PTEN*, whereas *VEGFR-1* and *VEGFR-2* were grouped together and closely positioned to all effectors of the PI3K/Akt pathway (*PIK3CA*, *PIK3CB*, *PDPK1*, *AKT1*, and *AKT2*).

### Mutation Analysis

Mutation analysis of *K-RAS* identified 2 amino acid-changing (missense) point mutations in 2 different tumors and a splice variant in all thyroid samples, including the normal thyroid glands. A G12R substitution (GGT > CGT) was present in 1 FTC of compact type and an E63K substitution (GAG > AAG) was observed in 1 MTC (Fig 4). In the *K-RAS* splice variant, exon 2 was missing.

Mutation analysis of *N-RAS* showed 1 silent mutation in codon 138 (GGG > GGA) in 2 FTC of compact type, occurring in heterozygous form.

Mutation analysis of *H-RAS* showed 1 silent mutation in codon 47 (GAC > GAT) in 21 FTC and 5 MTC occurring in both homozygous and heterozygous forms.

Mutation analysis of *BRAF* did not identify any point mutations. However, a splice variant in which exons 13 and 14 were missing was present in all samples, including normal thyroid glands.

Mutation analysis of *PIK3CA* and *RET* did not show any abnormalities in the sequenced region.

Mutation analysis of the entire coding region of *PTEN* showed 1 silent mutation in codon 325 (CTC > CTT) in 5 FTC and 3 MTC, occurring in both homozygous and heterozygous form.

### Discussion

Information on the genetic events leading to thyroid cancer in dogs is scarce. In our study, mRNA expression of several genes involved in the PI3K/Akt signaling pathway was increased in canine FTC and MTC

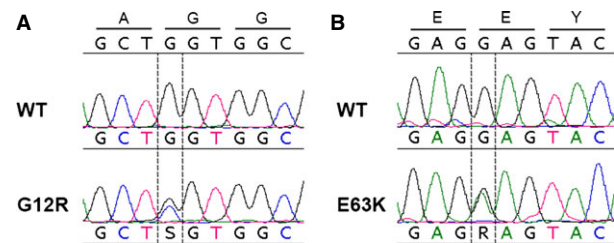


**Fig 4.** Mutations found in codon 12 of *K-RAS* (A) in a canine FTC and in codon 63 of *K-RAS* (B) in a canine MTC. WT, wild type; FTC, follicular cell thyroid carcinoma; MTC, medullary thyroid carcinoma.

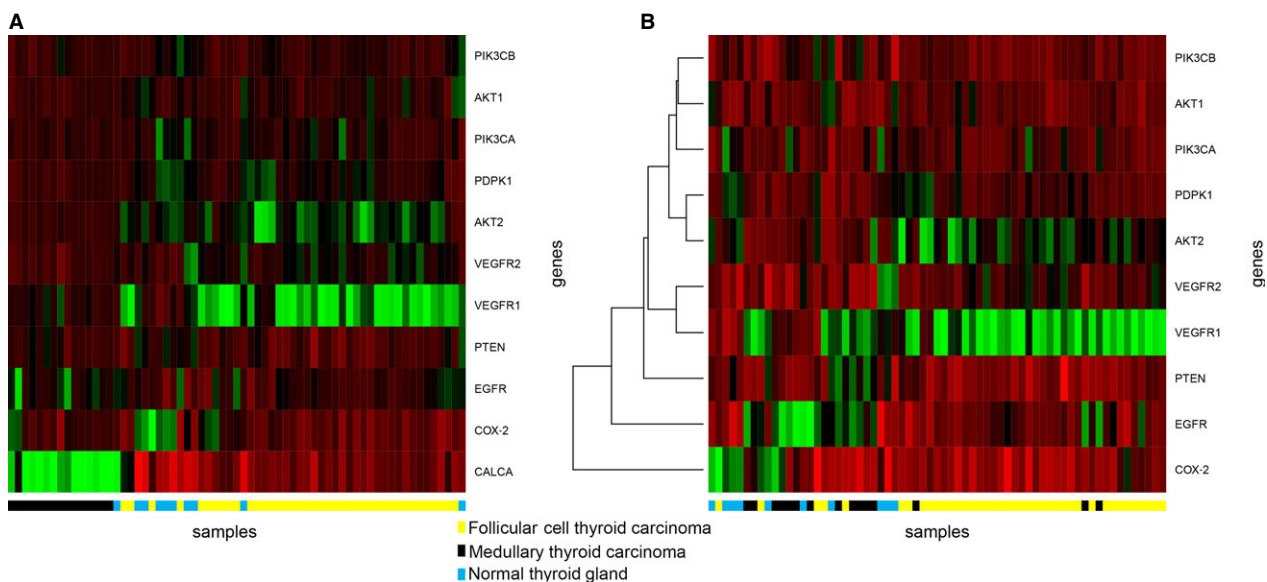


**Fig 3.** Heat maps illustrating the results of the unsupervised hierarchical clustering in canine normal thyroid gland ( $n = 10$ ), follicular cell thyroid carcinoma ( $n = 41$ ), and medullary thyroid carcinoma ( $n = 15$ ). (A) All genes included in the analysis. (B) Relative expression of calcitonin omitted from the analysis.

when compared to normal thyroid gland, and missense mutations of *K-RAS* were found in 1 FTC and 1 MTC. These findings support the role of the PI3K/Akt signaling pathway in the tumorigenesis of thyroid carcinoma in dogs.

In humans, gene amplification can lead to activation of cancer-related signaling pathways and plays an important role in thyroid gland tumorigenesis.<sup>5</sup> In our study, overexpression of *VEGFR-1*, *VEGFR-2*, *PDPK-1*, *AKT1*, and *AKT2* in canine FTC and overexpression of *VEGFR-1*, *EGFR*, and *PIK3CA* in canine MTC suggest activation of PI3K/Akt pathway, particularly in FTC. The PI3K/Akt pathway therefore could play an important role in canine thyroid tumorigenesis promoting cell proliferation, resistance to apoptosis, and malignant transformation.<sup>29</sup> Mechanisms responsible for the upregulation of the above mentioned genes include gene amplification and altered promoter activity.<sup>6</sup>

The 2 missense mutations in *K-RAS* identified in our study also have been reported in thyroid cancer of humans with a similar prevalence. The G12R substitution observed in a compact FTC has been described in 1 of 24 follicular thyroid carcinomas and in 3 of 108 sporadic MTC without *RET* mutation in humans.<sup>30,31</sup>

Regulation of RAS protein function occurs through intrinsic guanosine triphosphatase (GTPase) activity, which in the wild-type *RAS* switches the protein from an active (guanosine triphosphate[GTP]-bound) to an inactive (guanosine diphosphate [GDP]-bound) state. The substitution of an amino acid without a side chain (glycine) in position 12 by another amino acid with a side chain (arginine), interferes with the geometry of the protein, impeding hydrolysis of GTP by GTPase.<sup>32</sup> Such mutations in *RAS* lead to a permanently activated protein and downstream signaling, facilitating uncontrolled cell division and tumor growth.<sup>33</sup>

The E63K substitution observed in MTC also has been described in 1 of 16 MTC without *RET* mutation in humans.<sup>34</sup> This mutation affects an evolutionarily conserved amino acid residue identical in all RAS proteins. Similarly to what is described for G12R substitution, the change of glutamic acid in position 63 to lysine also has been demonstrated to abolish GTPase activity, leading to constitutive activation of RAS and potentiating cellular transformation.<sup>35</sup>

No amino acid-changing mutations were found in the sequenced regions of *H-RAS*, *N-RAS*, *BRAF*, *PIK3CA*, and *RET* nor in the entire coding sequence of *PTEN*. Hence, the mutations most commonly involved in thyroid tumorigenesis in humans are rare and do not play a major role in the pathogenesis of thyroid carcinoma in dogs.

The absence of mutations in the sequenced region of *RET* in 16 MTC is in agreement with a case report of familial MTC in 3 dogs in which no mutations were found after complete sequencing of *RET*.<sup>19</sup> Additional research is needed to investigate the genetic events involved in the pathogenesis of canine MTC.

Splice variants of *K-RAS* and *BRAF* were observed in all thyroid tumors. However, given their presence in

normal thyroid gland tissue, these are unlikely to play a role in thyroid gland tumorigenesis in dogs.

Involvement of the PI3K/Akt pathway in the pathogenesis of thyroid carcinoma in dogs suggests this pathway may constitute a promising therapeutic target. The importance of PI3K/Akt pathway activation and the value of targeting this pathway recently have been demonstrated in several canine cancer cell lines.<sup>36</sup> Furthermore, a preliminary study in dogs with solid tumors showed that toceranib phosphate, a multitargeted TKI which targets VEGFR-2, was associated with a clinical benefit rate of 80% in 15 dogs with thyroid carcinoma.<sup>37</sup> In humans with unresectable, radioiodine-refractory thyroid cancer, TKIs and inhibitors of PI3K/Akt signaling have shown encouraging results in recent clinical trials.<sup>38</sup>

Despite the overexpression of many PI3K/Akt-related genes suggesting pathway activation, the relative expression of *COX-2* was not increased in thyroid tumors in dogs. Similar findings have been reported in human follicular thyroid carcinoma, in which PI3K/Akt pathway activation is of major importance.<sup>39</sup> This suggests that mRNA expression of *COX-2* may not reflect activation of PI3K/Akt signaling in thyroid cancer.

As expected, canine FTC and MTC showed distinct mRNA expression profiles of PI3K/Akt pathway-related genes. These differences were confirmed by unsupervised clustering and suggest that these tumor types probably arise by different molecular mechanisms. The fact that mRNA expression of *CALCA* did not overlap between FTC and MTC confirms the accuracy of tumor classification based on IHC for calcitonin.

In our study, sequencing of human mutation hotspots was performed to investigate the presence in dogs of the most common mutations involved in thyroid cancer in humans. This approach was adopted over sequencing the entire coding region and regulatory regions of each gene because of its efficiency to achieve our goal.

Limitations of our study include the lack of protein data when interpreting mRNA expression levels because mRNA and protein expression do not always correlate. Furthermore, our findings of increased expression of RTKs and intracellular effectors involved in PI3K/Akt signaling warrant further research on phosphorylation of Akt (pAkt) and other members of this pathway to verify pathway activation.

In conclusion, overexpression of *VEGFR-1*, *VEGFR-2*, *PDPK-1*, *AKT1*, and *AKT2* in canine FTC and *VEGFR-1*, *EGFR*, and *PIK3CA* in canine MTC suggests that the PI3K/Akt signaling pathway is activated and likely involved in the pathogenesis of thyroid cancer in dogs, especially in FTC. The mRNA expression of *CALCA* did not overlap between canine FTC and MTC. Two missense mutations in *K-RAS* were identified in an FTC and an MTC which are likely to be relevant for thyroid gland tumorigenesis. The mutations most frequently associated with thyroid cancer in humans are rare in dogs.

---

## Footnotes

- <sup>a</sup> Dako, Glostrup, Denmark  
<sup>b</sup> Qiagen, Hilden, Germany  
<sup>c</sup> NanoDrop Technologies, Wilmington, DE  
<sup>d</sup> Agilent Technologies, Santa Clara, CA  
<sup>e</sup> Bio-Rad, Hercules, CA  
<sup>f</sup> Eurogentec, Maastricht, The Netherlands  
<sup>g</sup> New England BioLabs Inc, Ipswich, MA  
<sup>h</sup> Applied Biosystems, Carlsbad, CA  
<sup>i</sup> Amersham, Buckinghamshire, UK  
<sup>j</sup> DNASTAR, Madison, WI  
<sup>k</sup> GraphPad Prism 6.03, GraphPad Software Inc, La Jolla, CA  
<sup>l</sup> R 3.0.2, R Foundation for Statistical Computing, Vienna, Austria
- 

## Acknowledgments

The authors thank the Department of Pathobiology of Utrecht University for providing all paraffin-embedded tumor samples of patients diagnosed and treated at Utrecht University and the Department of Morphology of Ghent University for sectioning the paraffin-embedded tumor samples. The authors also thank Prof. Dr Luc Duchateau of the Department of Comparative Physiology and Biometrics of Ghent University for his assistance in statistical analysis.

This research was supported by the ECVIM-CA Clinical Studies Fund and the Special Research Fund of Ghent University (grant no. 01J02510).

*Conflict of Interest Declaration:* The authors disclose no conflict of interest.

## References

- Loar AS. Canine thyroid tumors. In: Kirk RW, ed. *Current Veterinary Therapy IX*. Philadelphia, PA: WB Saunders Co; 1986:1033–1039.
- Wucherer KL, Wilke V. Thyroid cancer in dogs: An update based on 638 cases (1995–2005). *J Am Anim Hosp Assoc* 2010;46:249–254.
- Harari J, Patterson JS, Rosenthal RC. Clinical and pathologic features of thyroid tumors in 26 dogs. *J Am Vet Med Assoc* 1986;188:1160–1164.
- Patnaik AK, Lieberman PH. Gross, histologic, cytochemical, and immunocytochemical study of medullary thyroid carcinoma in sixteen dogs. *Vet Pathol* 1991;28:223–233.
- Xing M. Molecular pathogenesis and mechanisms of thyroid cancer. *Nat Rev Cancer* 2013;13:184–199.
- Liu Z, Hou P, Ji M, et al. Highly prevalent genetic alterations in receptor tyrosine kinases and phosphatidylinositol 3-kinase/akt and mitogen-activated protein kinase pathways in anaplastic and follicular thyroid cancers. *J Clin Endocrinol Metab* 2008;93:3106–3116.
- Gerber HP, McMurtrey A, Kowalski J, et al. Vascular endothelial growth factor regulates endothelial cell survival through the phosphatidylinositol 3'-kinase/Akt signal transduction pathway. Requirement for Flk-1/KDR activation. *J Biol Chem* 1998;273:30336–30343.
- Hynes NE, Lane HA. ERBB receptors and cancer: The complexity of targeted inhibitors. *Nat Rev Cancer* 2005;5:341–354.
- Chen W, Bai L, Wang X, et al. Acquired activation of the Akt/cyclooxygenase-2/Mcl-1 pathway renders lung cancer cells resistant to apoptosis. *Mol Pharmacol* 2010;77:416–423.
- Ladu S, Calvisi DF, Conner EA, et al. E2F1 inhibits c-Myc-driven apoptosis via PIK3CA/Akt/mTOR and COX-2 in a mouse model of human liver cancer. *Gastroenterology* 2008;135:1322–1332.
- Usher SG, Radford AD, Villiers EJ, et al. RAS, FLT3, and C-KIT mutations in immunophenotyped canine leukemias. *Exp Hematol* 2009;37:65–77.
- Malumbres M, Barbacid M. RAS oncogenes: The first 30 years. *Nat Rev Cancer* 2003;3:459–465.
- Xing M. Genetic alterations in the phosphatidylinositol-3 kinase/Akt pathway in thyroid cancer. *Thyroid* 2010;20:697–706.
- Cohen Y, Xing M, Mambo E, et al. BRAF mutation in papillary thyroid carcinoma. *J Natl Cancer Inst* 2003;95:625–627.
- Hofstra RM, Landsvater RM, Ceccherini I, et al. A mutation in the RET proto-oncogene associated with multiple endocrine neoplasia type 2B and sporadic medullary thyroid carcinoma. *Nature* 1994;367:375–376.
- Salvatore D, Melillo RM, Monaco C, et al. Increased in vivo phosphorylation of ret tyrosine 1062 is a potential pathogenetic mechanism of multiple endocrine neoplasia type 2B. *Cancer Res* 2001;61:1426–1431.
- Cerrato A, De Falco V, Santoro M. Molecular genetics of medullary thyroid carcinoma: The quest for novel therapeutic targets. *J Mol Endocrinol* 2009;43:143–155.
- Moura MM, Cavaco BM, Pinto AE, et al. High prevalence of RAS mutations in RET-negative sporadic medullary thyroid carcinomas. *J Clin Endocrinol Metab* 2011;96:E863–E868.
- Lee JJ, Larsson C, Lui WO, et al. A dog pedigree with familial medullary thyroid cancer. *Int J Oncol* 2006;29:1173–1182.
- Kiupel M, Capen C, Miller M, et al. Histological classification of the endocrine system of domestic animals. In: Schulman FY, ed. *WHO International Histological Classification of Tumors of Domestic Animals*. Washington, DC: Armed Forces Institute of Pathology; 2008:25–39.
- Campos M, Ducatelle R, Kooistra HS, et al. Immunohistochemical expression of potential therapeutic targets in canine thyroid carcinoma. *J Vet Intern Med* 2014;28:564–570.
- Brinkhof B, Spee B, Rothuizen J, et al. Development and evaluation of canine reference genes for accurate quantification of gene expression. *Anal Biochem* 2006;356:36–43.
- Galac S, Kool MM, Naan EC, et al. Expression of the ACTH receptor, steroidogenic acute regulatory protein, and steroidogenic enzymes in canine cortisol-secreting adrenocortical tumors. *Domest Anim Endocrinol* 2010;39:259–267.
- Schmittgen TD, Livak KJ. Analyzing real-time PCR data by the comparative C(T) method. *Nat Protoc* 2008;3:1101–1108.
- Vasko V, Ferrand M, Di Cristofaro J, et al. Specific pattern of RAS oncogene mutations in follicular thyroid tumors. *J Clin Endocrinol Metab* 2003;88:2745–2752.
- Xing M, Westra WH, Tufano RP, et al. BRAF mutation predicts a poorer clinical prognosis for papillary thyroid cancer. *J Clin Endocrinol Metab* 2005;90:6373–6379.
- Samuels Y, Wang Z, Bardelli A, et al. High frequency of mutations of the PIK3CA gene in human cancers. *Science* 2004;304:554.
- Minaguchi T, Yoshikawa H, Oda K, et al. PTEN mutation located only outside exons 5, 6, and 7 is an independent predictor of favorable survival in endometrial carcinomas. *Clin Cancer Res* 2001;7:2636–2642.
- Osaki M, Oshimura M, Ito H. PI3K-Akt pathway: Its functions and alterations in human cancer. *Apoptosis* 2004;9:667–676.

30. Ciampi R, Mian C, Fugazzola L, et al. Evidence of a low prevalence of RAS mutations in a large medullary thyroid cancer series. *Thyroid* 2013;23:50–57.
31. Hong HH, Houle CD, Ton TV, et al. K-ras mutations in lung tumors and tumors from other organs are consistent with a common mechanism of ethylene oxide tumorigenesis in the B6C3F1 mouse. *Toxicol Pathol* 2007;35:81–85.
32. Scheffzek K, Ahmadian MR, Kabsch W, et al. The Ras-RasGAP complex: Structural basis for GTPase activation and its loss in oncogenic Ras mutants. *Science* 1997;277:333–338.
33. Richter A, Murua Escobar H, Gunther K, et al. RAS gene hot-spot mutations in canine neoplasias. *J Hered* 2005;96:764–765.
34. Boichard A, Croux L, Al Ghuzlan A, et al. Somatic RAS mutations occur in a large proportion of sporadic RET-negative medullary thyroid carcinomas and extend to a previously unidentified exon. *J Clin Endocrinol Metab* 2012;97:E2031–E2035.
35. Quilliam LA, Hisaka MM, Zhong S, et al. Involvement of the switch 2 domain of Ras in its interaction with guanine nucleotide exchange factors. *J Biol Chem* 1996;271:11076–11082.
36. Chen YT, Tan KA, Pang LY, et al. The class I PI3K/Akt pathway is critical for cancer cell survival in dogs and offers an opportunity for therapeutic intervention. *BMC Vet Res* 2012;8:73.
37. London C, Mathie T, Stingle N, et al. Preliminary evidence for biologic activity of toceranib phosphate (Palladia(R)) in solid tumours. *Vet Comp Oncol* 2012;10:194–205.
38. Liebner DA, Shah MH. Thyroid cancer: Pathogenesis and targeted therapy. *Ther Adv Endocrinol Metab* 2011;2:173–195.
39. Fuhrer D, Eszlinger M, Karger S, et al. Evaluation of insulin-like growth factor II, cyclooxygenase-2, ets-1 and thyroid-specific thyroglobulin mRNA expression in benign and malignant thyroid tumours. *Eur J Endocrinol* 2005;152:785–790.
40. Nikiforov YE, Nikiforova MN. Molecular genetics and diagnosis of thyroid cancer. *Nat Rev Endocrinol* 2011;7:569–580.